https://doi.org/10.4322/cobramseg.2022.1030
ISBN: 978-65-89463-30-6

XX Congresso Brasileiro de Mecânica dos Solos e Engenharia Geotécnica
IX Simpósio Brasileiro de Mecânica das Rochas
IX Simpósio Brasileiro de Engenheiros Geotécnicos Jovens
VI Conferência Sul Americana de Engenheiros Geotécnicos Jovens
XI Congresso Luso Brasileiro de Geotecnia
23 a 26 de Agosto de 2022 – Campinas – SP

COBRAMSEG 2022
23 A 26 DE AGOSTO | CAMPINAS | SP | BRASIL
COBRAMSEG | SBMR | GEOJOVEM | CLBG

Three-dimensional numerical modeling for analysis of failure events at the base of inclined pillars

Jaime Andres Corredor Herrera
Geotechnical UG, Rio Tinto, Canada. Jaime.CorredorHerrera@riotinto.com

ABSTRACT: The study area is characterized by a tabular to lenticular quartz vein with an average thickness of 1.5 m, gently dipping 20 °, extracted by the room and pillar mining method. In a certain location of the mine, the first evidence of floor puncture features was identified, represented mostly by cracks and protrusions longitudinal and oblique to the sills of the production drifts, followed by statements of spontaneous mass loss in the pillars. A detailed review of the geological information made possible to formulate a relationship between the unstable region and a local 5-meter-thick layer of Talc schist underneath the base of the pillars. The deformations, failures and settlements of sill and pillar base in this low strength rock mass was then compared to the concepts of load-bearing capacity for shallow squared foundations in Soils. due to the particularities of the excavation formats such as shanty back drifts, asymmetric, and anisotropic pillars, the study performed a strain–stress analysis by three-dimensional finite element numerical modeling, to offer a closer estimate of the behaviors observed in the field.

KEYWORDS: Room and Pillar, Bearing capacity, 3D numerical modeling, Talc Schist, Floor Punching.

1 Introduction

The interaction between pillars and their surroundings is a very important factor in mine stability analyses explored through the room and pillar mining method. When the rock mass materials of the base of the pillars are weak or susceptible to rapid, significant deterioration, regional stability of the mine may be conditioned by floor behavior, rather than the characteristics of the pillars or back strata. Depending on the depth, the misinterpretation of the expected ground behavior may result in massive collapse, or even trigger large-scale subsistence processes.

Specific research devoted to the room and pillar design formulate a series of calculations, such as stable spans and strength of the natural support pillars (Lunder and Pakalnis, 1997, Martin and Maybee, 2000), are now considered as classical methods in rock mechanics. These works consider the effect of intact rock strength and fracture patterns associated with the rock mass characterization, however, focus on the stability of the back or integrity of the pillar core, leaving the behavior of failure mechanisms of the sills shallow or no rock mechanics assessment.

During the production stages of the study mine site, fast and intense deformation processes began manifesting on the sill of the drifts and pillars of a specific sector of the mine. The studied panel is located at 120 meters depth, 180 meters long along the strike, and affects about 50 mining pillars and 4 barrier pillars.

A comprehensive review of the geological information of the sector of interest made it possible to formulate a close relationship between the instabilities with a local 5-meter-thick layer of Talc schist at the base of the pillars. This lithology was mapped on a more detailed scale and geomechanically parameterized using empirical field techniques and more sophisticated methods like GSI (Hoek, 2001).

ISBN: 978-65-89463-30-6

2 Methods

The discussion of hard rock pillar design using the tributary area method assumes that the loading capacity for the host rock is limited to the strength of the ore layer (Brady et al., 2004). In cases where low-strength rock mass is in the floor (or occasionally in the roof), the support pillar system will collapse by punching the pillar to its base; This type of event is always accompanied by floor swelling in adjacent drifts, as is the case of foundations in soil.

Salmia et al. (2017) state that when floor materials are weak or vulnerable to extensive deterioration, overall mine stability is controlled by the behavior of the floor than the mechanical responses of the pillars or overload strata. Cases of subsidence on the surface are also expected, usually due to pillar settlement and their puncture in the less resistant strata on the floor.

In practice, a pillar laying over a soft rock on the floor can be compared to a shallow rectangular foundation in soil. Therefore, the theory of foundation bearing capacity can be applied to the analysis of interactions between a hard rock pillar and soft floor materials. Proposals made by Wyllie (2005) and Salmia et al. (2017) show that the uniaxial compressive strength of a rock mass on the floor can be considered as the ultimate load capacity of the rock. Therefore, the stresses on a certain pillar should be contrasted with the load capacity of the floor strata to assess its stability, a characteristic that herein is more significant than the stresses of the pillar, this statement will be the focus of further analysis.

When applied loads are much smaller than the ultimate load capacity, the rock mass will behave elastically. However, larger loads reaching the final load capacity of the rock mass could trigger the formation of cracks, which eventually grow, intersect each other, contributing to the formation of wedges and crushed rock. These conditions will result in rock dilation. Figure 1 shows that the rock under a theoretical squared pillar base is in a biaxial compression state, with the major principal stress σ_{1A} equal to the ultimate load capacity and the minimum principal stress is equal to the confinement applied to the surrounding rock.

The reduced strength of the rock under the pillar compared to the surrounding rock is illustrated in Figure 2. The maximum stress that the surrounding rock can sustain is the uniaxial compressive strength of the rock mass $\sigma_{u(m)}$ in zone B. The analysis assumes active and passive wedges, defined by straight lines in the rock under the pillar, and the shear strength parameters of these surfaces are those of the rock mass. The maximum principal stress in zone A, σ_{1A}, is equal to the load of the pillar, if the weight of the rock below ground is disregarded. Zone B assumes the largest main effort σ_{1B} acting horizontally, and the smallest main effort σ_{3B} acting vertically. If the base is on the ground surface, σ_{3B} is zero. Regarding the base rupture, both zones shear simultaneously, and the smallest main stress in zone A, σ_{3A}, is equal to the main stress zone B, σ_{1B}.

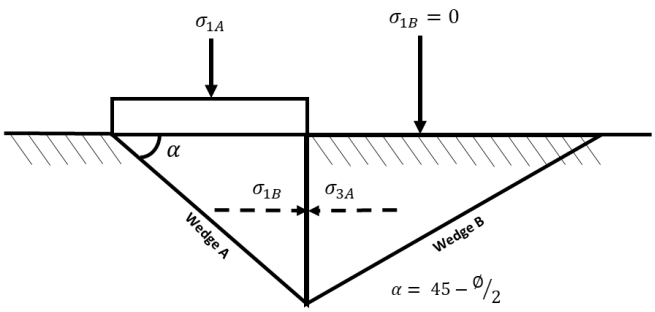

Figure 1. Stress field schematics for load-bearing capacity of foundations over a fractured rock: Active wedge A, passive wedge B (Modified from Wyllie, 2005).

ISBN: 978-65-89463-30-6

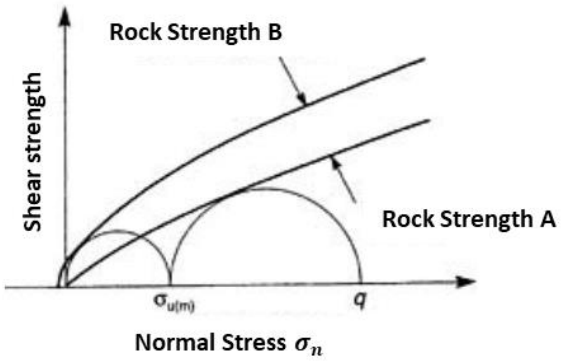

Figure 2. Decreased rock strength under the pillar compared to surrounding rock (Wyllie, 2005).

The calculation of the very fractured or very weak rock loading capacity, based on the failure mechanism of Figure 1 is largely oversimplified, since it assumes planar failure surfaces, ignoring the rock weight at the base as well as the shear stresses that develop along with the vertical interface between both wedges. Therefore, it could be considered that analytical methodologies are not fully applicable to foundation failure problems.

2 Materials

In the case study area, the deformation manifests differently according to lithology. For the back and pillar composed of intercalated schists, they are presented in layers with an average thickness of +10 meters, characterized as good to regular quality rock mass, with uniaxial compressive strength values ranging from 100 to 125 MPa. Small fractured intervals may arise due to discontinuities (failures or fractures). Floor composed locally of Schist Talc with Quartz and Sericite, as a 5-meter-thick layer, is characterized by a regular to bad quality rock mass, having uniaxial compressive strength values around 20 MPa. Several field tests show that this unit has similar physical properties to intact rock when confined but has important changes, such as constant breaks in the foliation plane, disintegrating on contact with water, which provides conditions for the formation of a soft and clayey material.

Observations in the underground drifts show that the material varies greatly in strength. In some locations, especially in the study area, resistance is as low as 1 to 5 MPa. In addition, there are friction angles of +/- 15 degrees as determined by simple field trials. The input data for lithologies are presented in Table 1.

Table 1. Rock mass deformability parameters From GSI classification values.

Parameters	Intercalated Schist	Talc Schist
UCS	123	28
GSI	52	30
Mi	14.0	7.7
Cohesion (MPa)	7.0	1.1
Friction Angle (°)	34	26
Tensile Strength (MPa)	-0.24	-0.04
Equivalent Strength (MPa)	26.3	3.5
Poisson	0.38	0.41
Young Modulus (MPa)	15907	2491

These values are stored as design input values to be applied or designated as properties of the different geometries, polygons, and volumes that are created to represent the spatial distribution of the geological elements that will compose the initial model. Due to data processing capacity limitations, it is assumed that this is a continuous model. The influence of discontinuities associated to the foliation has been already considered on the GSI values, whereupon these values are assumed as the mechanical and elastic properties for equivalent rock masses.

ISBN: 978-65-89463-30-6

3 Three-dimensional model

This section is of key importance in the model building since it is where the excavation geometries and dimensions of the excavations are defined, which will be the spatial representation of the model, the intersections of the excavations with the different geological elements of the model, the number of stages to be analyzed and the materials of each geometry to be designated. Details of the initial configuration of the model are presented in Figures 3 and 4.

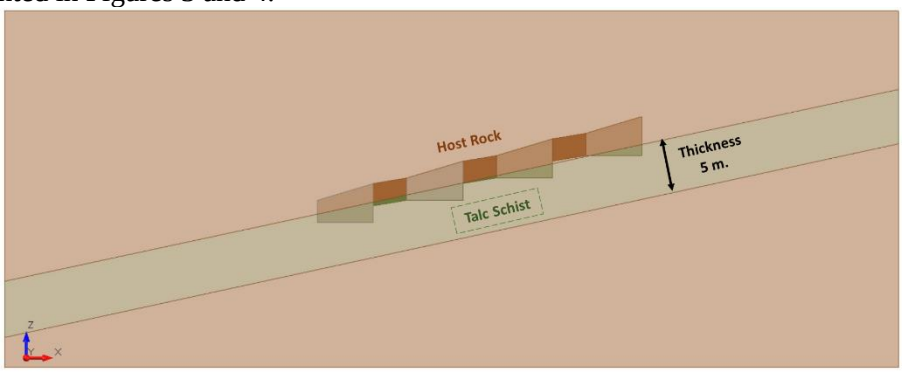

Figure 3. Geometry proposed for the industry geology, the Talc Schist layer (in green) is 5 meters thick.

For the mesh generation, the software provided a simplified default set up, consisting in tetrahedral, 4-node graded elements, that populated the surroundings of the excavation with small-size elements, gradually increasing its size as the spatial location was closer to the model boundaries.

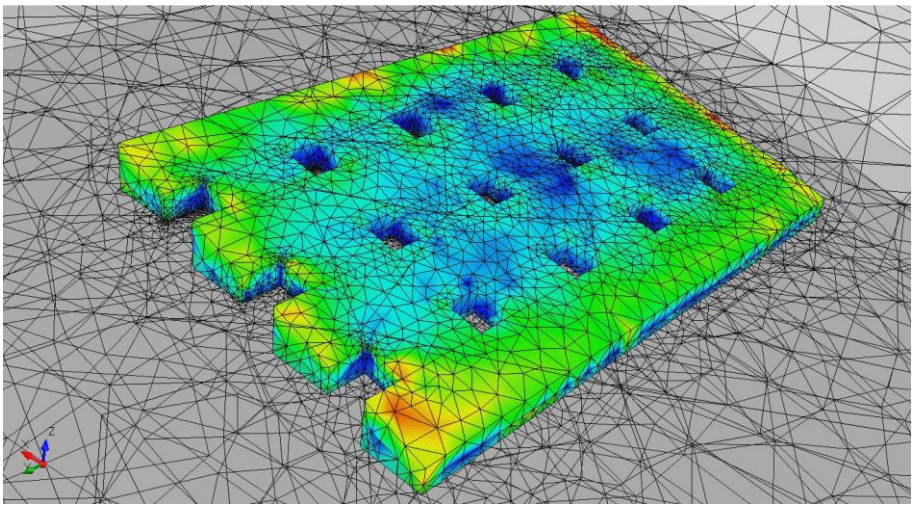

Figure 4. View of the excavation discretization result at the end of the mining sequence.

4 Calibration

To verify how the result of the final model will behave considering all the uncommon variables that compose the study framework (Larger horizontal stress, diverse lithologies, inclined layers and complex geometries), the author chooses to run an initial model simplifying the parameters to a single lithology and comparing them with study results or related examples. For this, the results performed by Suorineni *et al*. (2011) are shown below.

The homogeneous model performed as calibration scenario, is set up to compare the stress distribution obtained from numerical finite element analysis for homogeneous pillars (composed by the same lithology in sill, pillar body and back) in an inclined position (Figure 5a). Although the inclinations presented in both models are different, the purpose of Suorineni *et al*. (2011) was to show the asymmetric distribution of induced stresses when submitted to a shear regime in a symmetric, inclined pillar (assumed square) and composed by a single lithology, presenting stress concentration zones (overload) and relaxation zones (deconfinement) at specific

ISBN: 978-65-89463-30-6

and diametrically opposite points of the pillar. The two zones produce unfavorable effects on the stability of the pillar (Figure 5b).
No information is officially reported regarding the determination of the main stress field in the study mine site; herein we chose to work with a horizontal stress rate 2.5 times the magnitude of the vertical effort due to the calculation of the excavation design in an isotropic environment, varying the magnitude of the k-value of 1.0, 1.5, 2.0 and 2.5. This last one presents shear stress and magnitude closer to the expected models (Suorineni *et al*., 2011).

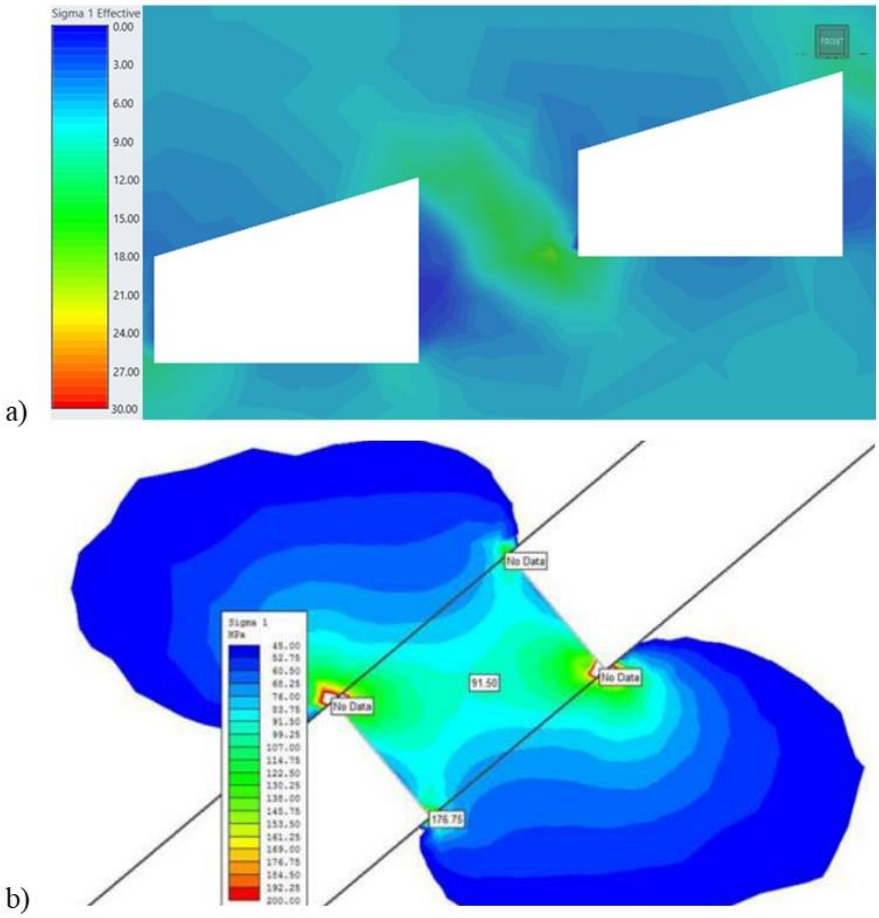

Figure 5: Major main effort distribution for homogeneous inclined pillars; a) This study; b) Suorineni *et al*. (2011)

From this observation it can be concluded that not only the parameters of rock and mass resistance should be considered in the analysis, but also that the configuration of the model already induces shear stress in the analysis, and therefore in the results.

5 Results

During the development stage, the accumulated stresses (Figure 7a) around the entire excavation are shown; As excavations increase, stresses on the back and floor decrease and are transmitted to the excavation edges, but mainly to the pillars; there is a concentration of stress on the contacts with the back in the lower gallery and the contact with the upper gallery floor and pillar body; the oblique arrangement of the concentration regions indicates shear-type solicitation;. the deconfinement regions (blue) on the sides of the drifts are highlighted (Figure 7a).

ISBN: 978-65-89463-30-6

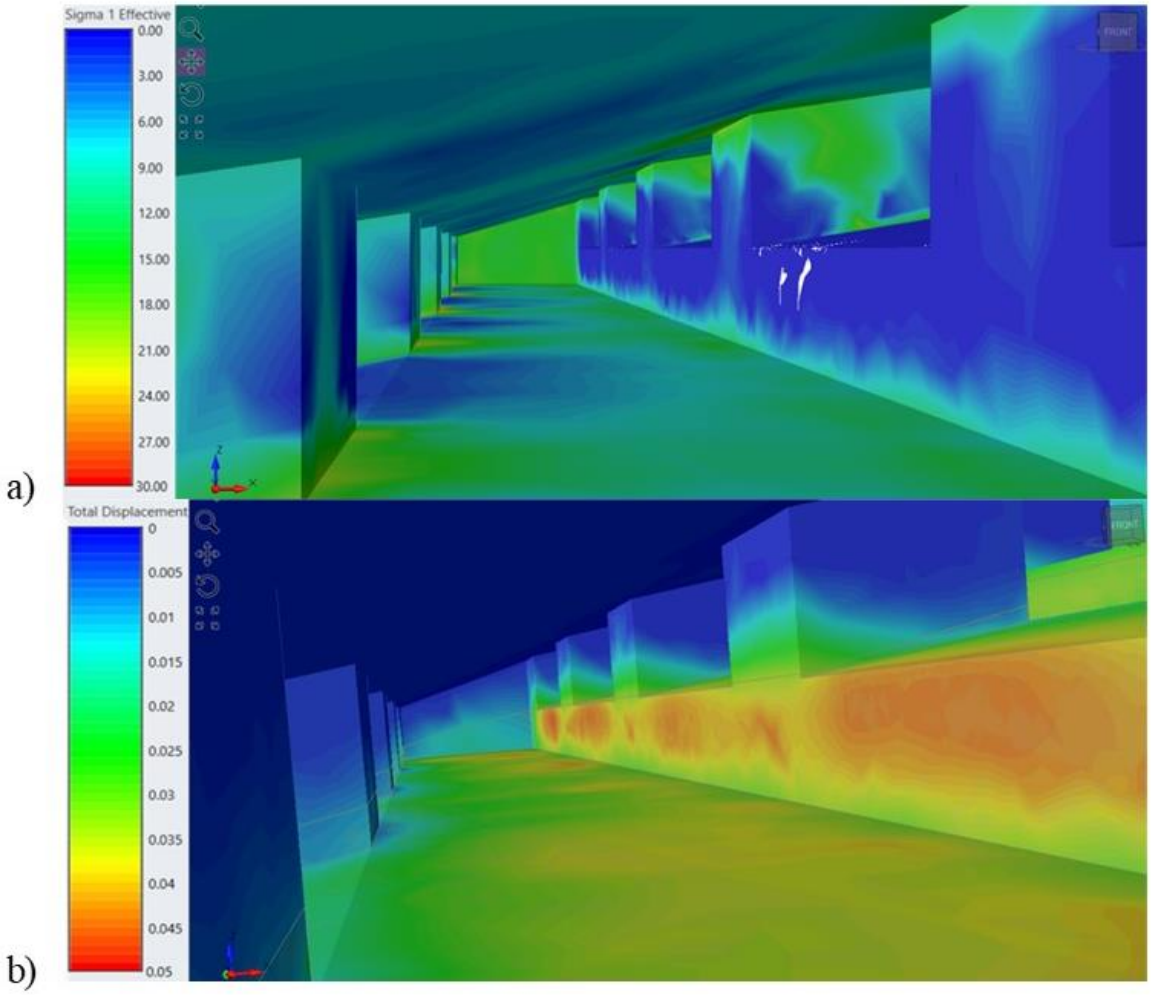

Figure 6. a) Distribution of σ_1 for inclined pillars; b) resulting from the measured effort on a vertical section of the central pillar.

ISBN: 978-65-89463-30-6

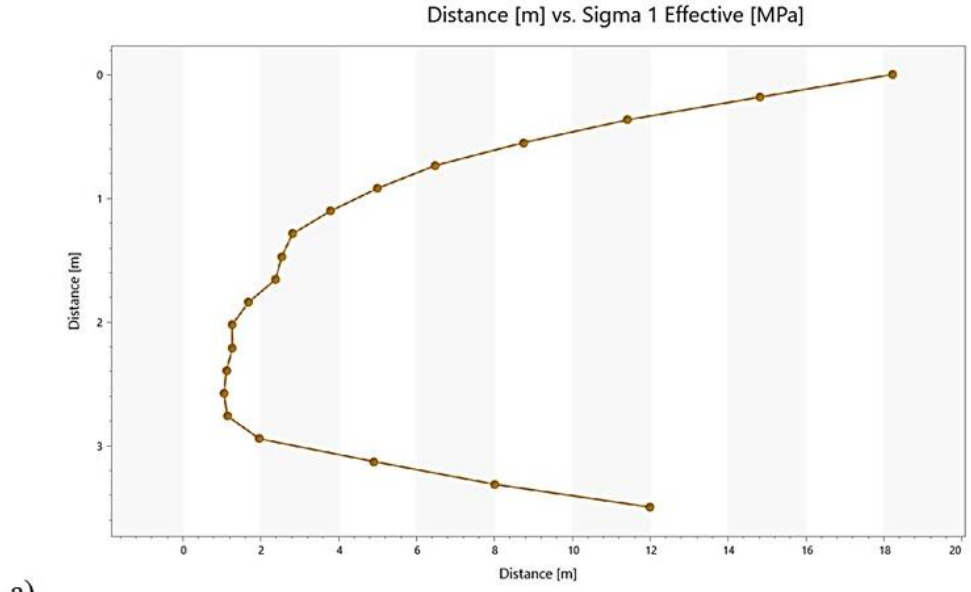

a)

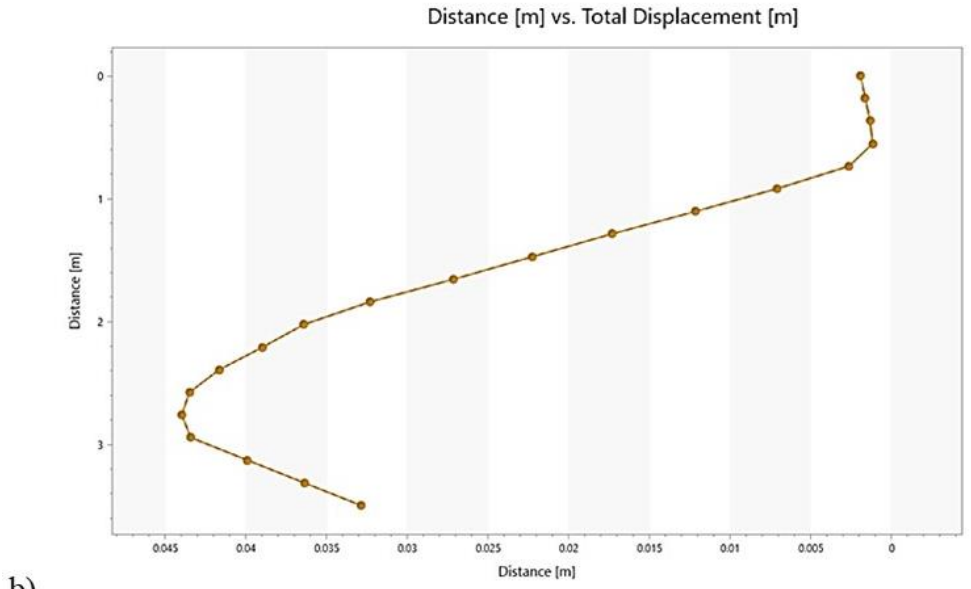

b)

Figure 7. a) Resultant displacement for inclined pillars along the sill of the excavation; b) Resultant displacement measured on a vertical section of one of the pillars.

For the resulting displacement, the model in Figure 7a shows a high contrast in the response of displacement values along the lithological contact. The lateral displacement is evident in the footwall portions exposed between pillars even from the early stages. The displacement recorded in the floor is less intense but is increasing as the excavation progresses. No displacement in the back or pillar contact is recorded. There is a significant displacement from the development stage and the regions of greater displacement are delimited along the lithological contact between the pillars. The displacement contours converge at the base of the pillar and concentrate to a greater extent at the base of the upper sides of the drifts.

6 Discussion

To understand the results, the study focused on the type of break presented in a schematic stratified geological model. This makes the following observations possible:
The Schist talc layer in the study region is stratigraphically concordant at the base of the mineralized layer, but in the study region it seems to approach until it comes into direct contact with the ore. In this region, the thickness of the Schist talc layer could be greater than in the rest of the mine sectors.

ISBN: 978-65-89463-30-6

The tensioning stress of the pillars reached the point where it exceeded the last load capacity of the schist talc layer at the base of the pillars, causing the floor punching phenomena, therefore the foundation failure directly below the pillars. This action creates tensile stresses at the bottom and middle of the pillars, which causes pillars to be deformed, especially along the lithological contact exposed at the pillar edge.

7 Conclusions

The pillars are part of a system that incorporates the back and floor immediately adjacent to itself; by increasing the deconfinement associated with excavation and mining, stresses extend to the floor and ceiling. The behavior of the base of the stratified pillars is an integral part of the overall behavior of the system, which is why it should be included in the design analysis from the feasibility phase.

In the model for stratified pillars, there are punching-type ruptures, so stability is controlled in these sectors by the geomechanical properties of the Schist Talc layers at the base.

In the modeling results, punching and mass loss can be appreciated in limited situations without causing the total breakage of the pillar. Thus, the breakage of the pillar happens from a new scenario created by the punching mechanism, resulting in shear failure.

The contrast between a high modulus material and very low modulus material has been shown to induce stress concentration. This is the triggering cause of failure of the Schist Talc pillars at the base.

ACKNOWLEDGEMENTS

Special thanks to Professor André Pacheco Assis for the technical and logistical support, To Leandro Ribes De Lima and Jairo Henrique da Silva for the technical review and field work cooperation, to Albert Cabrejo and Antonio Rocha from *GroundProbe*® Brasil and *RocScience*® South America, and specially to Eng. Glauber Rosa Luvizotto.

REFERENCES

Brady, Barry H.G.; Brown, Ted. *Rock Mechanics for Underground Mining.* 3. ed. Dordretch: Kluwer Academic Publishers, 2004. 628 p.

Hoek, Evert. Rock mass properties for underground mines. in: Underground Mining Methods: Engineering Fundamentals and International Case Studies. 3. ed. Littleton, Colorado: Society for Mining, Metallurgy, and Exploration, 2001.

Lunder, P. J.; Pakalnis, R. C. *Determination of the strength of hard-rock mine pillars*. CIM Bulletin, Littleton, Colorado, v. 90, n. 1013, p. 51-57, 1997.

Martin, C.; Maybee, W. *The Strength of Hard Rock Pillars*. International Journal of Rock Mechanics and Mining Sciences, [s. l.], v. 37, p. 1239-1246, 2000.

Salmia, E. F.; Nazemb, M.; Karakusc, M. *The effect of rock mass gradual deterioration on the mechanism of postmining subsidence over shallow abandoned coal mines*. International Journal of Rock Mechanics & Mining Sciences, [s. l.], v. 91, p. 59–71, 2017.

Suorineni, F.; Kaiser, P.; Thibodeau, D. *Mining of orebodies under shear loading: part 1 - case histories.* Transactions of the Institution of Mining and Metallurgy, Section A: Mining Technology, [s. l.], v. 120, n. 137, 2011.